BIOCHEMISTRY
including biophysical chemistry & molecular biology

ARTICLE

pubs.acs.org/biochemistry

Direct Observation of the Structural Change of Tyr174 in the Primary Reaction of Sensory Rhodopsin II

Misao Mizuno,[†,⊥] Yuki Sudo,[‡,§,⊥] Michio Homma,[‡] and Yasuhisa Mizutani*[,†]

[†]Department of Chemistry, Graduate School of Science, Osaka University, 1-1 Machikaneyama, Toyonaka, Osaka 560-0043, Japan
[‡]Division of Biological Science, Graduate School of Science, Nagoya University, Chikusa-ku, Nagoya 464-8602, Japan
[§]PRESTO, Japan Science and Technology Agency (JST), 4-1-8 Honcho, Kawaguchi, Saitama 332-0012, Japan

Supporting Information

ABSTRACT: Sensory rhodopsin II (SRII) is a negative phototaxis receptor containing retinal as its chromophore, which mediates the avoidance of blue light. The signal transduction is initiated by the photoisomerization of the retinal chromophore, resulting in conformational changes of the protein which are transmitted to a transducer protein. To gain insight into the SRII sensing mechanism, we employed time-resolved ultraviolet resonance Raman spectroscopy monitoring changes in the protein structure in the picosecond time range following photoisomerization. We used a 450 nm pump pulse to initiate the SRII photocycle and two kinds of probe pulses with wavelengths of 225 and 238 nm to detect spectral changes in the tryptophan and tyrosine bands, respectively. The observed spectral changes of the Raman bands are most likely due to tryptophan and tyrosine residues located in the vicinity of the retinal chromophore, i.e., Trp76, Trp171, Tyr51, or Tyr174. The 225 nm UVRR spectra exhibited bleaching of the intensity for all the tryptophan bands within the instrumental response time, followed by a partial recovery with a time constant of 30 ps and no further changes up to 1 ns. In the 238 nm UVRR spectra, a fast recovering component was observed in addition to the 30 ps time constant component. A comparison between the spectra of the WT and Y174F mutant of SRII indicates that Tyr174 changes its structure and/or environment upon chromophore photoisomerization. These data represent the first real-time observation of the structural change of Tyr174, of which functional importance was pointed out previously.

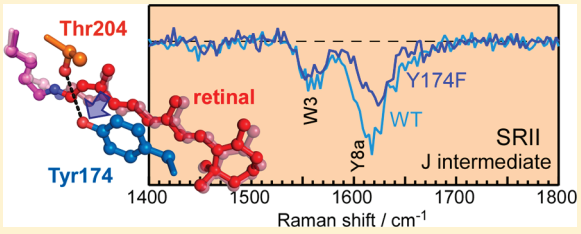

Sensory rhodopsin II (SRII, also called phoborhodopsin, pR)[1] is a member of an archaeal rhodopsin family and serves as a negative phototaxis receptor in archaea such as *Natronomonas pharaonis* and *Halobacterium salinarum*. SRII can be activated by blue light (~500 nm) and positively regulates the phosphorylation of a kinase CheA during the photocycle, which induces the rotation change of the flagellar motor through the phosphorylated response regulator CheY, resulting in negative phototaxis from harmful near-UV light. SRII has seven transmembrane α-helices and forms the signaling complex with its cognate transducer protein, HtrII, in the membrane. The chromophore, *all-trans*-retinal, binds to a lysine residue through a protonated Schiff base and is surrounded by the helices. This feature is commonly found among microbial rhodopsins such as the outwardly light-driven proton pump bacteriorhodopsin (BR), the inwardly light-driven Cl^- pump halorhodopsin (HR), and sensory rhodopsin I (SRI, also called sensory rhodopsin, sR), which is a sensor of both negative and positive phototaxis.[2,3] Light absorption of microbial rhodopsins triggers trans−cis photoisomerization of retinal chromophores, leading to protein conformational changes that are essential to their functions. The conformational changes are followed by cyclic chemical reactions consisting of several sequential intermediate states (J, K, L, M, N, and O). The structure and function of BR have been extensively studied, and as a result, BR is one of the best understood membrane proteins. However, considerably less is known about the structure and function of other microbial rhodopsins.

The structures of SRII and its complex with HtrII have been studied by X-ray crystallography[4,5] and various other spectroscopic methods.[1,2,6] With regard to the primary process of the photocycle, structural differences between the original state and the cryogenically trapped photointermediates have been deduced from FTIR studies[7−10] and X-ray diffraction on protein crystals.[11] The primary chromophore reaction dynamics of SRII are quite similar to those of BR.[12,13] The early photointermediates, J, K, and KL, which exhibit red-shifted absorption bands relative to the original state, have been defined by time-resolved measurements. The formation time constants of the J and K states are approximately 0.5 and 3 ps, respectively.[12] However, little is known about the temporal evolution of the SRII protein structure.

Determining the structural dynamics of protein moiety associated with its chromophore at ambient temperature is key to elucidating the signal transduction mechanism. Although the

Received: November 12, 2010
Revised: March 8, 2011
Published: March 14, 2011

signaling state of SRII is believed to be the long-lived M state, which appears in the microsecond time range, ultrafast protein responses must be studied in order to understand the coupling between retinal isomerization and protein conformational changes as well as how the M state evolves following photoisomerization. Gross et al.[14] recently succeeded in measuring femtosecond infrared spectra of SRII, but they were unable to assign the observed spectral changes to specific amino acid residues or specific peptide units.

Time-resolved ultraviolet resonance Raman (UVRR) spectroscopy probes protein structural dynamics at specific sites by selectively enhancing the vibrational bands attributable to tryptophan and tyrosine residues.[15,16] The pump−probe method using pulses in the picosecond range is preferable for the study of ultrafast protein dynamics. We constructed a picosecond time-resolved UVRR system and used it to elucidate the structural dynamics of the ligand photodissociation of carbonmonoxy myoglobin,[17,18] the primary protein response of photoactive yellow protein,[19] and the photoinduced electron transfer of glucose oxidase.[20] Most recently, we reported picosecond time-resolved UVRR spectra of the J, K, and KL states of BR.[21]

In the present study, we investigated the primary protein response to retinal isomerization of SRII in the early intermediates on the basis of picosecond time-resolved UVRR spectra. We chose two probe wavelengths to observe the vibrational bands due to each tryptophan and tyrosine residue. The time-resolved UVRR spectra clarified the structural changes that occur around the tryptophan and tyrosine residues located in the vicinity of the retinal chromophore. Most importantly, we succeeded in detecting structural and/or environmental changes of Tyr174, of which functional importance was pointed out previously,[8,22] taking the advantage that Raman band intensities of tyrosine residues in proteins are greatly enhanced in UV excitation.

EXPERIMENTAL PROCEDURES

Protein Expression and Purification. Wild type and Y174F mutant *Natronomonas pharaonis* SRII expression plasmids were constructed as previously described.[23] Cells were grown in LB medium supplemented with ampicillin (final concentration of 50 μg/mL). *E. coli* BL21(DE3) harboring each plasmid was grown to an OD_{660} of 0.3−0.4 in a 30 °C incubator, after which cells were induced by addition of 0.5 mM IPTG and 5 μM *all-trans*-retinal. Cells were harvested at 8 h postinduction at 18 °C by centrifugation at 4 °C, resuspended in buffer (50 mM MES, pH 6.5) containing 1 M NaCl, and disrupted by French press as previously described.[24] Cell debris was removed by low-speed centrifugation (5000*g*, 10 min, 4 °C). Crude membranes were collected by ultracentrifugation (100000*g*, 30 min, 4 °C) and washed with 50 mM MES, pH 6.5, containing 1 M NaCl. Membranes were solubilized by addition of 2% (w/v) *n*-dodecyl-β-D-maltoside (DDM) and incubation for 30 min at 4 °C. The solubilized membranes were isolated by ultracentrifugation (100000*g*, 30 min, 4 °C), and the supernatant was applied to a Ni-affinity column (HisTrap, GE Healthcare, Uppsala, Sweden) at 4 °C in the dark. The column was washed extensively with 50 mM MES, pH 6.5, containing 1 M NaCl, 20 mM imidazole, and 0.05% (w/v) DDM to remove nonspecifically bound proteins. The histidine-tagged proteins were then eluted using a linear gradient of up to 100% elution buffer (0.05% DDM, 1 M NaCl, 50 mM Tris-Cl, pH 7.0, and 500 mM imidazole). Eluted protein was then further purified by ion-exchange chromatography on a HiTrapQ column (GE Healthcare, Uppsala, Sweden) equilibrated with 50 mM Tris-Cl, pH 7.5, containing 30 mM NaCl and 0.05% DDM. The column was washed extensively with the buffer to remove nonspecifically bound proteins, and target proteins were eluted using a linear gradient of up to 100% elution buffer (0.05% DDM, 1 M NaCl, 50 mM Tris-Cl, pH 7.5). The sample medium was exchanged by Amicon Ultra (Millipore, Bedford, MA) filtration, and the samples were finally suspended in a buffer solution containing 150 mM NaCl, 50 mM Tris-HCl (pH 7.0), and 0.1% DDM.

Picosecond Time-Resolved UVRR Measurements. The experimental setup for picosecond time-resolved UVRR measurements has been described elsewhere.[18,19] Briefly, the light source for our apparatus was a picosecond-Ti:sapphire oscillator (Tsunami pumped by Millennia-Vs, Spectra-Physics) and amplifier (Spitfire pumped by Evolution-15, Spectra-Physics) system operating at 1 kHz. The wavelength and energy of the laser output were 796 nm and 800 μJ, respectively. Probe pulses of 225 and 238 nm were the second harmonic of the first Stokes line generated from CH_4 and H_2 Raman shifters, respectively, and were introduced into an etalon to reduce the spectral width. Another Raman shifter with compressed CH_4 gas generated pump pulses at 450 nm. The pump and probe pulses were collinearly overlapped and focused onto a flowing thin film of the sample solution by a planoconvex lens. Typical pulse energies were 8 μJ (pump) and 0.5 μJ (probe) at the sample point. Chromophore absorption was bleached by a maximum of 26% and 15% after 150 min time-resolved measurements of 40 and 100 μM samples, respectively. We calculated difference spectra to discuss spectral changes associated with the chromophore photoisomerization. Contribution of the bleached component to the raw spectra is canceled out in the difference spectra because the bleached component is not photoactive for 450 nm light. The zero-delay time was precisely determined by measuring the intensity of the difference frequency generation between the pump and probe pulses. The cross-correlation times between the pump and probe pulses were 3.5 ps (225 nm probe) and 3.4 ps (238 nm probe). The Raman scattering light was collected and focused onto the entrance slit of a Czerny-Turner configurated Littrow prism prefilter[25] coupled to a 50 cm single spectrograph (500M, SPEX) by two achromatic doublet lenses. The dispersed light was detected with a liquid nitrogen cooled CCD detector (SPEC-10:400B/LN, Roper Scientific). Raman shifts were calibrated with Raman bands of cyclohexane. The spectral dispersion was 3.0−3.5 cm^{-1}/pixel on the CCD detector. In the scan of delay time, the sequence of delay times was determined to be random. At each delay time, Raman signals were collected for three 20 s exposures with both pump and probe beams present in the sample. This was followed by equivalent exposures for pump-only, probe-only, and dark measurements. The transient Raman spectra were obtained by averaging the data for the repeated cycles. The sample bleaching is so slow that depletion of the intact component is negligible during one scan of delay time. Thus, this method enabled us to avoid errors caused by sample bleaching as well as slowly drifting laser power.

RESULTS

Time-Resolved 225 nm UVRR Spectra. The UVRR spectrum of SRII probed at 225 nm is shown in Figure 1. The top trace represents the UVRR spectrum of SRII in the original state. This spectrum contains all the Raman bands for the six tryptophan and

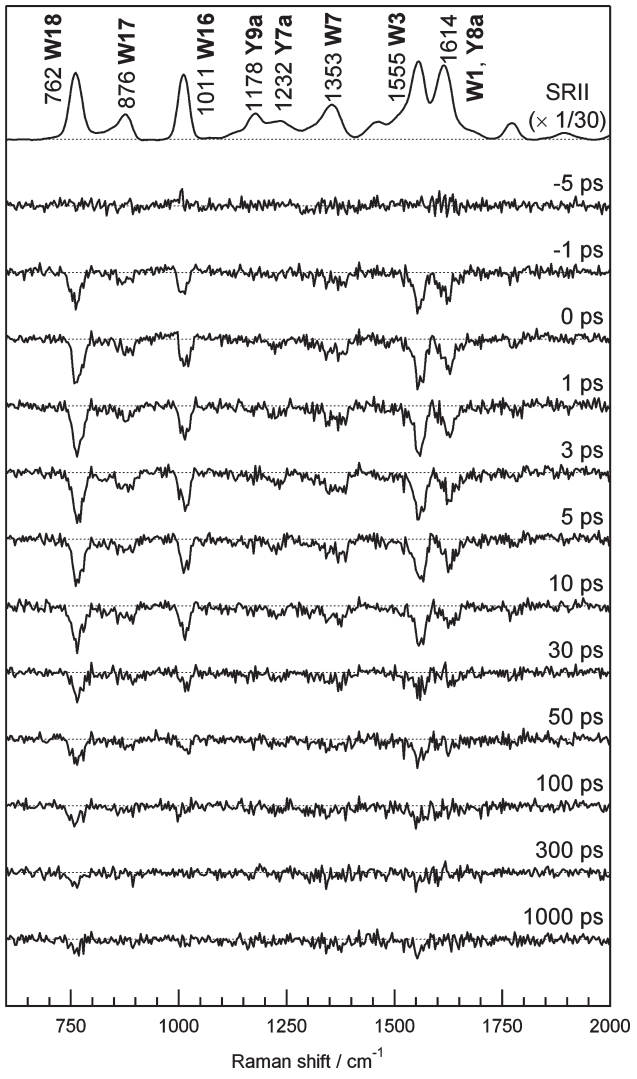

Figure 1. Picosecond time-resolved UVRR spectra of SRII. Probe and pump wavelengths are 225 and 450 nm, respectively. The top trace shows the probe-only spectrum divided by a factor of 30, representing the UVRR spectrum of SRII in the original state. The spectrum of the buffer has been subtracted. The remaining time-resolved difference spectra were generated by subtracting the probe-only spectrum from the pump−probe spectrum at each delay time shown. The accumulation time for obtaining each spectrum was 80 min. Vibrational normal modes and their descriptions of tryptophan and tyrosine are listed in Table S1 of the Supporting Information.

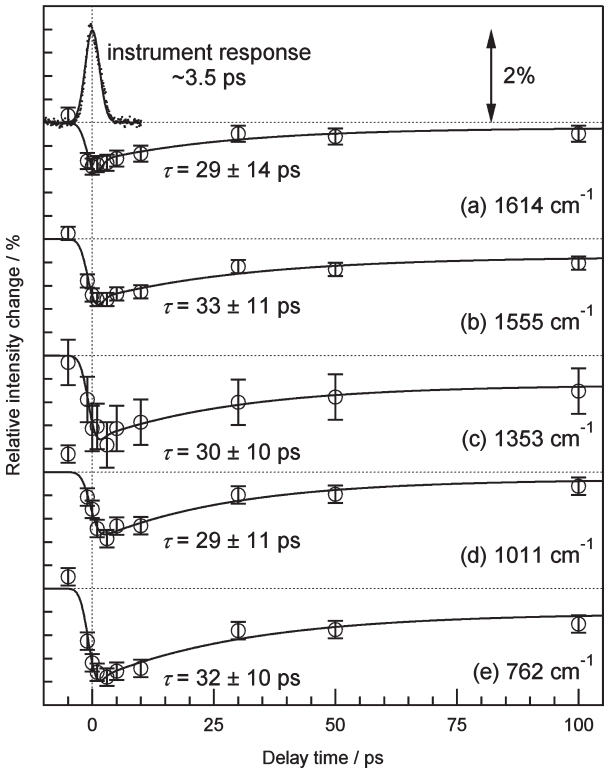

Figure 2. Temporal intensity changes of bands in time-resolved UVRR spectra taken with a 225 nm probe pulse: (a) 1614 cm^{-1} (the sum of W1 and Y8a); (b) 1555 cm^{-1} (W3); (c) 1353 cm^{-1} (W7); (d) 1011 cm^{-1} (W16); (e) 762 cm^{-1} (W18). Markers indicate the band intensity measured at each delay time relative to the intensity in the probe-only spectrum. Solid lines are the best fits of the function $[A_1 \times \delta(t) + A_2 \times \exp(-t/\tau) + A_3]$ convoluted with the instrument response function. The resulting parameter, τ, is indicated for each trace.

ten tyrosine residues in SRII. Vibrational bands of tryptophan and tyrosine side chains are noted as W and Y, respectively. The mode assignments made by Harada and Takeuchi[15] were adopted, and vibrational normal modes and their descriptions of observed tryptophan and tyrosine modes are listed in Table S1 of the Supporting Information. Tryptophan Raman bands dominate the spectrum probed at 225 nm because of the large Raman cross section arising from the strong electronic transitions to the B_a and B_b states.[26] Figure 1 also shows time-resolved UVRR difference spectra, obtained by subtracting the SRII spectrum in the original state from the spectrum measured at each delay time, ranging from −5 to 1000 ps. After photoexcitation, negative bands due to tryptophan residues were clearly observed within the instrument response time. The negative bands represent depletion of the Raman intensity resulting from the change in protein structure upon photoisomerization. At 3 ps, the intensity of the tryptophan bands decreased by about 1−2%. The negative bands decayed from 10 to 50 ps. This indicates that the tryptophan band intensity recovers due to further structural changes following the intensity depletion associated with photoisomerization. In the 100−1000 ps region the difference spectra did not change. No UVRR band for retinal was observed in the spectra; thus, the spectral change of the retinal chromophore did not contribute to the UVRR difference spectra. This is because the *all-trans*-retinal UVRR band intensity is much smaller than that of tryptophan under the resonance condition at 225 nm.[21]

The temporal intensity changes of five remarkable bands are shown in Figure 2. The 1614 cm^{-1} band can be attributed to the sum of the vibrational modes of tryptophan (W1) and tyrosine (Y8a). The bands at 1555, 1353, 1011, and 762 cm^{-1} were assigned to the vibrational modes of tryptophan residues W3, W7, W16, and W18, respectively. The temporal change of each band was well expressed by a curve with a function of $[A_1 \times \delta(t) + A_2 \times \exp(-t/\tau) + A_3]$, convoluted with the instrument response function. We found that the intensity of all bands instantaneously bleached within the instrumental response time and recovered with a time constant (τ) of ∼30 ps. The retinal chromophore isomerizes from the all-trans to the 13-cis form in 300−400 fs upon the formation of the primary photoproduct of the J state.[12] The initial UVRR intensity depletion can be

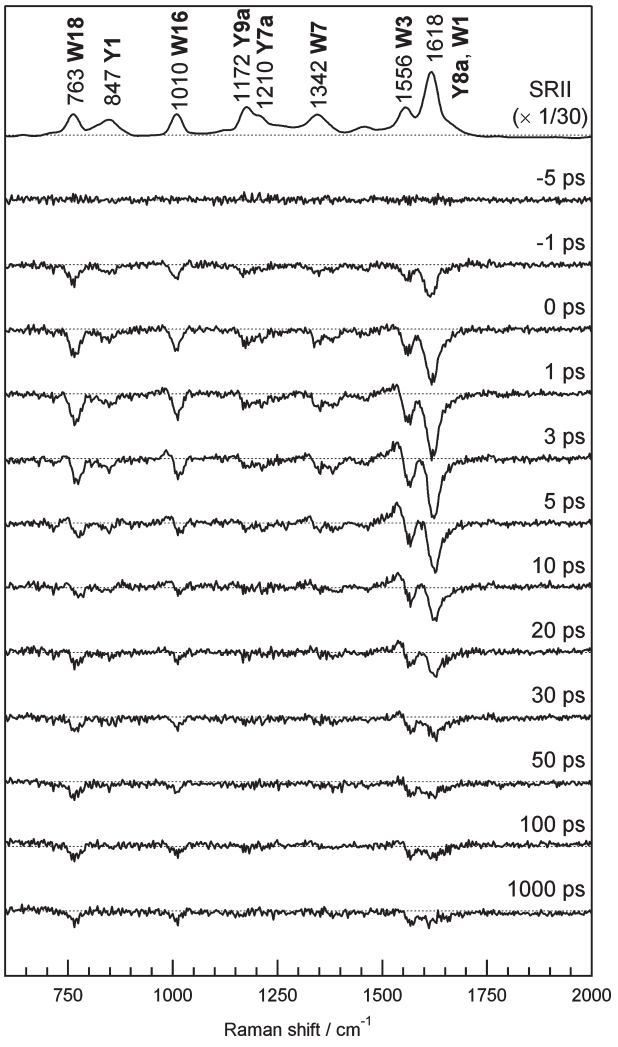

Figure 3. Picosecond time-resolved UVRR spectra of SRII. Probe and pump wavelengths are 238 and 450 nm, respectively. The top trace shows the probe-only spectrum divided by a factor of 30, representing the UVRR spectrum of SRII in the original state. The spectrum of the buffer has been subtracted. The remaining time-resolved difference spectra were generated by subtracting the probe-only spectrum from the pump−probe spectrum at each delay time shown. The accumulation time for obtaining each spectrum was 139 min. Vibrational normal modes and their descriptions of tryptophan and tyrosine are listed in Table S1 of the Supporting Information.

attributed to the protein's response to chromophore isomerization. The subsequent intensity recovery likely reflects protein response to the relaxation of the chromophore in SRII. Our results indicate that changes of protein structure in the SRII photocycle take place with a time constant of 30 ps, which is comparable to the time constant reported for the BR protein response.

Time-Resolved 238 nm UVRR Spectra. Figure 3 shows picosecond time-resolved UVRR spectra of SRII probed at 238 nm. The top trace represents the UVRR spectrum of SRII. The intensity of the tyrosine bands increase relative to the intensity of tryptophan bands probed at 238 nm because the Raman cross sections of the totally symmetric modes of tryptophan are significantly reduced under the resonance condition at this wavelength.[26] In the time-resolved difference spectra,

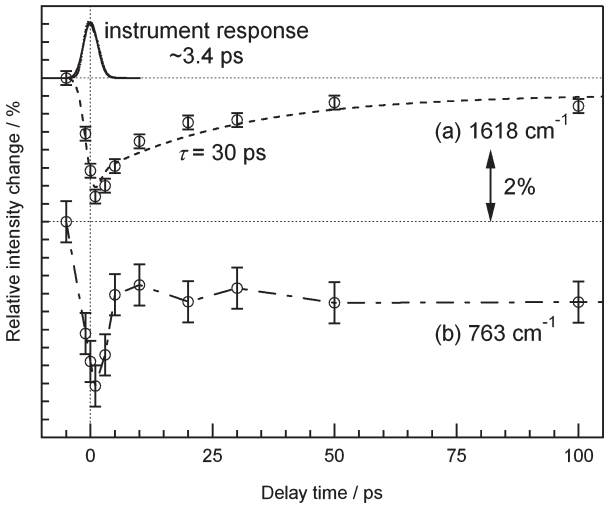

Figure 4. Temporal intensity changes of the (a) 1618 cm^{-1} (the sum of Y8a and W1) and (b) 763 cm^{-1} (W18) bands in time-resolved UVRR spectra taken with a 238 nm probe pulse over the −5 to 100 ps range. Markers indicate the band intensity measured at each delay time relative to the intensity in the probe-only spectrum. Broken line in trace (a) represents the simulated curves of the function $[A_1 \times \delta(t) + A_2 \times \exp(-t/\tau) + A_3]$ (the value of τ is fixed at 30 ps).

spectral changes in both the tryptophan and tyrosine bands were observed. Immediately after photoexcitation of the chromophore, the W3 band exhibited a sigmoidal form, indicating a wavenumber shift. The sigmoid form was observed up to 30 ps. The negative bands appeared at the position of the W16 and W18 bands, and the decrease in intensity is indicative of structural changes around the tryptophan residues. The pattern of the W16 and W18 bands in the difference spectra changed to the sigmoid form in 3−10 ps, indicating that the bands underwent a downshift. With regard to tyrosine, the negative Y8a band appeared within the instrument response time and decayed up to 30 ps. Similar to the 225 nm spectra, the contribution of the retinal chromophore to the spectral change was negligible in the difference spectra.[21]

Figure 4 shows the temporal behavior of the 1618 and 763 cm^{-1} bands. A broken line for the former indicates the curve with a function of $[A_1 \times \delta(t) + A_2 \times \exp(-t/\tau) + A_3]$, in which τ is fixed at 30 ps. The observed data points for the 1618 cm^{-1} band are well represented by the curves. The intensity of the band at 1618 cm^{-1}, assignable to the sum of the Y8a and W1 bands, decreased within the instrument response time and recovered with a time constant of 30 ps. This suggests that the 30 ps process detected under the 238 nm probe condition results from the protein response of SRII to chromophore isomerization, as was observed in the spectra probed at 225 nm. On the other hand, the temporal behavior of the W18 band in Figure 2e is different from that in Figure 4b, as it lost intensity faster than the 1618 cm^{-1} band. This suggests that the tryptophan residues responsible for the change observed between Figures 2 and 4 are different and also suggests that there is an additional process involved in the protein response of SRII to chromophore relaxation from that observed in the spectra probed at 225 nm. The observed spectral changes may therefore be attributable to at least two tryptophan residues. Such a fast recovery of UVRR band intensity was not observed for BR.[21]

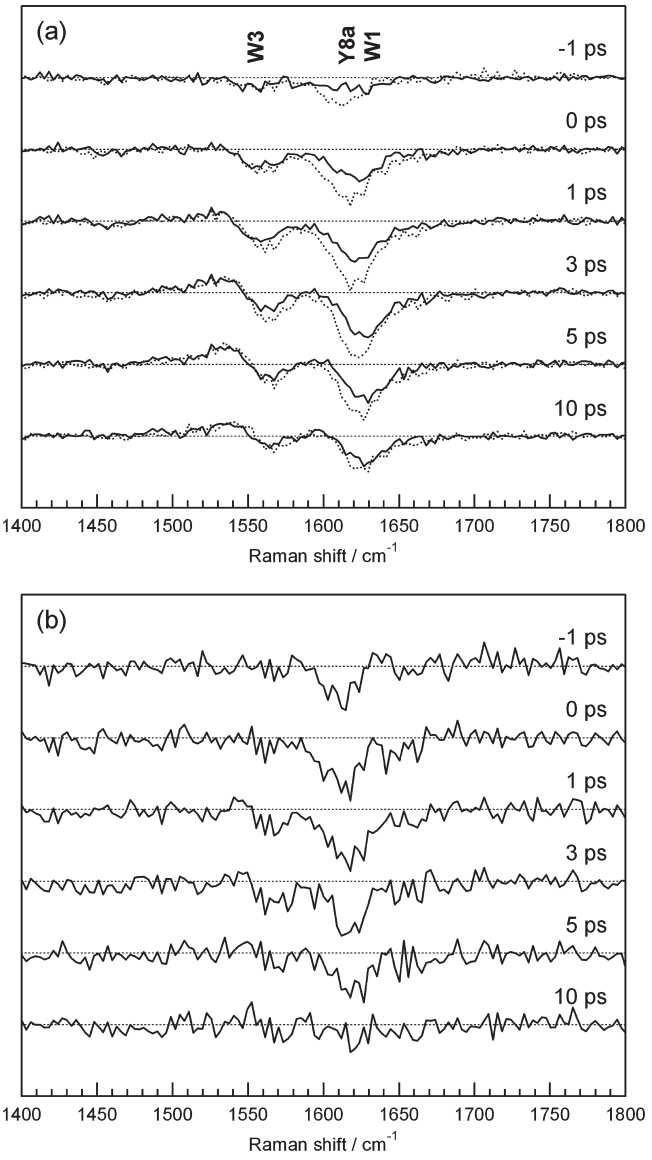

Figure 5. Picosecond time-resolved UVRR spectra of WT SRII and the Y174F mutant in the 1400−1800 cm^{-1} region. Probe and pump wavelengths were 238 and 450 nm, respectively. The accumulation times for obtaining WT and Y174F mutant spectra were 79 and 76 min, respectively. (a) Time-resolved difference spectra were generated by subtracting the probe-only spectrum from the pump−probe spectrum at each delay time shown. Solid and broken curves represent Y174F mutant and WT SRII spectra, respectively. (b) Time-resolved difference spectra between the time-resolved difference spectra of WT SRII and the Y174F mutant.

Time-Resolved UVRR Spectra of the Y174F Mutant. A comparison of the picosecond time-resolved UVRR spectra of WT SRII and the Y174F mutant probed at 238 nm is shown in Figure 5a. Solid and dotted curves in Figure 5a show the spectra of WT SRII and the W174F mutant, respectively. Spectral intensities were normalized to the band intensities of the W16 mode. In the time-resolved spectra, with regard to tryptophan bands, similar difference spectra were observed for the Y174F mutant and WT SRII. Immediately after photoexcitation of the chromophore, the W3 band exhibited a sigmoidal form because of a wavenumber shift, and this sigmoidal form was observed up to 30 ps. Negative bands appeared in positions corresponding to the W16 and W18 bands at 0 and 1 ps, and the decrease in intensity indicated structural changes had occurred around the tryptophan residues (see Supporting Information Figure S1 for wider wavenumber region spectra). The pattern of the two bands in the difference spectra changed to a sigmoid form in 3−20 ps, indicating that the bands underwent a downshift. It should be noted that the spectral features of all the tryptophan bands observed in the difference spectra were consistently close to those of WT SRII, indicating that the mutation does not significantly perturb the tryptophan residues. With regard to tyrosine bands, the negative Y8a band of the Y174F mutant appeared within the instrument response time and diminished in 1000 ps, similar to that of WT SRII. However, the negative bands of the Y8a mode in the Tyr174 spectra were much weaker than the corresponding bands in the WT spectra. This is strong evidence that Tyr174 is responsible for the intensity change of the Y8a band and that the structure and/or environment of Tyr174 changes in SRII following chromophore photoisomerization.

Figure 5b shows difference spectra between the time-resolved difference spectra of WT SRII and the Y174F mutant. These difference spectra correspond to the time-resolved spectra of the Tyr174 residue. The Y8a band bleached within the instrument response time and nearly recovered within 10 ps. The temporal behavior of the Y8a band shown in Figure 5b is similar to that of the fast recovering component of the 763 cm^{-1} band shown in Figure 4b.

DISCUSSION

Primary Photochemistry of SRII. Our time-resolved UVRR analysis of SRII provides structural information regarding the primary protein response associated with the photoreaction of the retinal chromophore. The primary chromophore reaction dynamics of SRII have been reported to be quite similar to the dynamics of BR.[12,13] Transient absorption data for SRII suggested that the excited electronic state decayed rapidly over 300−400 fs, initially to a red-shifted product state with subsequent formation of a second, less red-shifted product state over 4−5 ps.[12] The former and latter red-shifted states are designated as the J and K states, respectively. For BR, ultrafast vibrational spectroscopy[27−29] demonstrated that the retinal chromophore undergoes all-trans to 13-cis isomerization during relaxation from the electronic excited state to the J state in the hot ground state and that the chromophore is highly twisted about the C−C and C=C bonds of the polyene chain. The structural differences between the original and the K state of SRII have also been studied by static FTIR spectroscopy and X-ray diffraction of cryogenically trapped K state.[7,9,11,30] Moreover, the K state of SRII at low temperature is composed of two species whose absorption maxima are located at different wavelengths.[31] The presence of a KL-like state was suggested based on nanosecond photolysis measurements. Similarly to BR, the KL state appears only at room temperature. A time constant of the formation was found to be less than 50 ns.[13] The subsequent L state from the KL state is formed in about 0.99 μs.[13]

All the tryptophan bands probed at 225 nm (Figure 2), as well as the Y8a band in the 238 nm spectra (Figure 4), bleached within the instrumental response time. If the observed spectral change is brought about by structural changes induced by the K state formation, the time constant for which is 4−5 ps, the initial

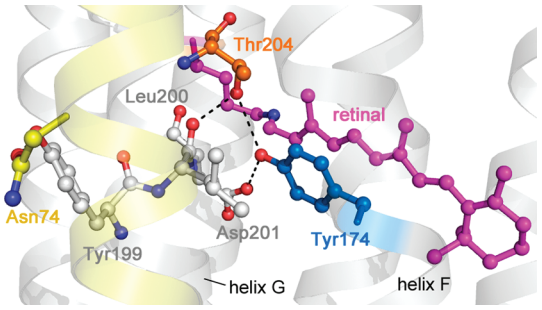

Figure 6. Details of the crystallographic structure of the SRII−HtrII complex in the original state (PDB ID: 1H2S[4]) in the vicinity of the chromophore, Tyr174, and Thr204. Black dashed lines indicate hydrogen bonds. The *all-trans*-retinal is bound to Lys205 via the protonated Schiff base linkage (magenta side chain). The helices of HtrII are in contact with the transmembrane helices F and G of SRII,[4] in which Tyr174 and Thr204 are involved, respectively. SRII Tyr199 is hydrogen-bonded to HtrII Asn74. The HtrII helix involving Asn74 is displayed by a yellow helix.

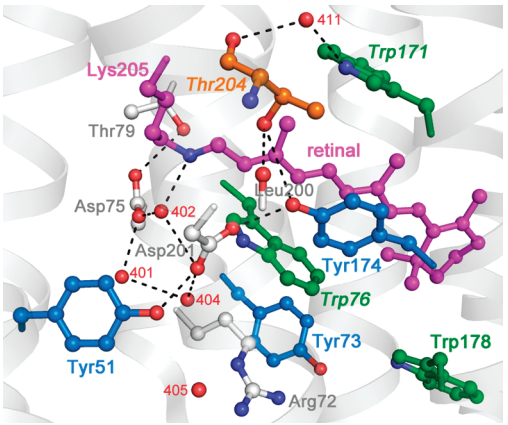

Figure 7. Crystallographic structure in the vicinity of the chromophore of SRII in the original state (PDB ID: 1JGJ[5]). Nitrogen and oxygen atoms are shown in blue and red, respectively. The magenta side chain represents the retinal chromophore and Lys205, which are linked through a protonated Schiff base. Green and cyan side chains represent tryptophans and tyrosines, respectively. Black dashed lines indicate hydrogen bonds. Italicized residues are located in the region 3.6 Å from the chromophore. Numerals 401, 402, 404, 405, and 411 indicate internal water molecules.

decrease in the intensity of these bands would be delayed compared to the instrumental response time. Accordingly, the initial intensity bleach most likely arises from the formation of the J state, which occurs over 300−400 fs. In addition, the negative bands in the UVRR difference spectrum at 10 ps can be attributed to bands of the K state spectrum because the J state is supposed to convert to the K state within 10 ps. The UVRR difference spectra due to the product of the 30 ps relaxation process from the K state can be assigned to the protein structure of the "post-K" state of SRII. The "post-K" state is presumably the KL state analogous to the case of BR photocycle.[21] The protein moiety does not necessarily instantaneously respond to the chromophore dynamics. The time constants of structural changes of the protein moiety observed by our UVRR spectroscopy can be different from those of retinal chromophore.

Structural Change of a Functionally Important Residue Tyr174. Assay measurements of SRII mutants showed that Tyr174 and Thr204 are key residues in the SRII signal transduction pathway.[22] Figure 6 shows the X-ray crystallographic structure of the SRII−HtrII complex around the two residues, which are located close to the retinal chromophore and form a hydrogen bond with each other.[23] The *all-trans*-retinal molecule binds to Lys205 via a protonated Schiff base linkage (magenta side chain). The HtrII helices are in contact with the SRII transmembrane helices F and G,[4] in which Tyr174 and Thr204, respectively, are located. One of the HtrII helices is displayed by a yellow helix. On the basis of the observation that phototaxis function was lost in Thr204 or Tyr174 mutants, Sudo et al. claimed that these residues are functionally important.[8] They also demonstrated the presence of steric constraint between the $C_{14}H$ group and Thr204 using FTIR spectroscopy.[32] Furthermore, the extent of the steric constraint correlated with the physiological phototaxis response.[8] Sudo et al. therefore proposed that the light signal is transmitted to HtrII from the energized interhelical hydrogen bond between Thr204 and Tyr174. The energized hydrogen bond is located both in the retinal chromophore pocket and in helices F and G that form the membrane-embedded interaction surface and is transmitted to the signal-bearing second transmembrane helix (TM2) of HtrII.[33] Thus, while the roles of SRII Thr204 in structural changes and in negative phototaxis are clearly understood, the role of Tyr174 in these processes is not.

To date, there has been no direct evidence indicating that the structure and/or environment of Tyr174 changes following chromophore photoisomerization. However, our data clearly show that the structure and/or environment of Tyr174 does change following chromophore photoisomerization. If the steric constraint between the $C_{14}H$ group and Thr204 is present, its effect would be exerted on Tyr174 simultaneously with photoisomerization. In fact, as Figure 5b shows, the contribution of Tyr174 to the Y8a band intensity was observed immediately upon photoisomerization. Thus, the present data are consistent with the model described above. We cannot rule out the possibility that the UVRR difference spectra of the Y174F mutant contain contribution of the protein structure of the O-like state, which was observed in the low-temperature FTIR spectra of Y185F mutant of BR.[34] However, it is highly likely that there is no difference between reactions of WT and Y174F SRII in the picosecond region because the temporal evolutions of spectral changes in the other tyrosine and tryptophan bands are almost the same in the WT and Y174F spectra.

Tyr174 is located in the extracellular portion of helix F. It is thought that the photoreaction of SRII in complex with HtrII induces an outward movement of the cytoplasmic portion of helix F,[35] which in turn triggers a rotation of HtrII TM2.[36] Interestingly, the functional importance of the light-induced outward tilting of helix F has been reported for also BR[37,38] as well as SRII.[35,36] The sequence of Tyr174 and Pro175 in SRII is conserved in all microbial rhodopsin in the tilting of helix F in response to retinal isomerization. In BR, it is conserved as the sequence of Tyr185 and Pro186.[39] The structural change in Tyr174 may act as a trigger for the movement of helix F.

Tryptophan and Tyrosine Residues Responsible for the Spectral Changes. Tryptophan and tyrosine residues change their structures in the vicinity of retinal during the early picosecond time frame. Figure 7 shows the amino acid residues and internal water molecules included in the hydrogen-bond network

around the retinal-binding pocket.[5] The hydrogen bonds are displayed by black dashes. The side chains of several residues are located in a region that lies close to (within 3.6 Å) the polyene chain or the β-ionone ring of retinal. Among the six tryptophan residues in SRII, Trp76, Trp171, and Trp178 are close to the chromophore. Trp76 and Trp171 sandwich the polyene chain of the retinal molecule, and Trp171 is oriented toward the 9- and 13-methyl groups of retinal, indicating that there is strong steric repulsion between the side chain of Trp171 and retinal. Trp178 is positioned near the β-ionone ring. Trp171 is also hydrogen-bonded to the main-chain oxygen atom of Thr204 via water molecule 411, while Trp76 is close to the pentagonal cluster near the Schiff base region. The cluster is generally believed to play an important role in the pumping mechanism of BR. The pentagonal cluster structure, together with two deprotonated aspartic acids (Asp75 and Asp201) and three internal water molecules (401, 402, and 404), is preserved in the Schiff base region of SRII.

Three of ten tyrosine residues (Tyr51, Tyr73, and Tyr174) exist in the retinal-binding pocket. Tyr174 is oriented parallel to and in close proximity to the polyene chain of retinal as described earlier. Both Tyr51 and Tyr174 are hydrogen-bonded to the deprotonated Asp201 residue involved in the hydrogen-bond network in the active site. All other tryptophan (Trp9, Trp24, and Trp60) and tyrosine (Tyr36, Tyr37, Tyr85, Tyr124, Tyr139, Tyr140, and Tyr199) residues are located very far from the polyene chain of the chromophore (>10 Å). With the exception of Tyr36 and Tyr37, these residues are located at the surface of the protein. It is reasonable to assume that the three tryptophan (Trp76, Trp171, and Trp178) and three tyrosine (Tyr51, Tyr73, and Tyr174) residues are responsible for the spectral change demonstrated in the present study.

For the early intermediates of BR, the structural changes occurring in the chromophore and in its vicinity have been studied by ultrafast time-resolved Raman[27,29,40−44] and infrared[28,45−50] spectroscopic measurements taken at room temperature and by cryospectroscopic[51−60] and crystallographic[61,62] measurements as well as molecular dynamics calculations.[63,64] These studies suggested that, in the intermediate states appearing in the picosecond time frame at ambient temperature, photoisomerization and the twist about the skeletal bonds of the polyene chain lead to significant changes in protein structure in the Schiff base region rather than in the area surrounding the β-ionone ring. This may also be the case with SRII. Therefore, Trp76 and Trp171, which are located close to the retinal polyene chain, are the residues most likely responsible for the spectral change we observed. Tyr51 and Tyr174 are the most likely residues to exhibit the spectral change because these residues participate in the hydrogen-bond network that includes the protonated Schiff base.

We previously reported spectral changes in tryptophan and tyrosine residues following chromophore isomerization in picosecond time-resolved UVRR spectra of BR.[21] The spectral changes were tentatively assigned to Trp86, Trp182, Tyr57, and Tyr185, all of which are located in the vicinity of the chromophore. Interestingly, all of these BR residues are conserved in SRII. The respective SRII counterparts are Trp76, Trp171, Tyr51, and Tyr174. Especially, it is reasonable that Tyr174 undergoes the structural change during the early stages of the photocycle because low-temperature FTIR studies of BR mutants of Y185F reported that structural changes of Tyr185 directly couple with retinal isomerization.[65,66]

Changes in Protein Structure around the Tryptophan Residue. On the basis of the spectral changes in the structural marker bands in the UVRR difference spectra, we now discuss the primary protein structural changes occurring around the tryptophan residues. On the basis of the spectral changes of some marker bands, it has been suggested that there is a reduction in hydrophobicity around tryptophan residues in the photointermediates of BR.[21] Similar spectral changes were observed in the early picosecond time frames for SRII. In both the 225 nm (Figure 1) and 238 nm (Figure 3) time-resolved UVRR difference spectra, negative bands appeared at the positions of the W16 and W18 bands, implying that the intensities of these bands bleached following photoisomerization. These bands are attributable to the indole breathing modes.[15] The Raman intensity of the W16 and W18 modes is enhanced in resonance with the B_a and B_b states.[67,68] The absorption band of the B_b transition is blue-shifted when the hydrophobicity around the tryptophan residue is reduced.[69,70] The shift of the absorption band accompanies the shift of the Raman excitation profile and thus influences resonance enhancement of the Raman bands. The maximum of the tryptophan Raman excitation profile locates around 225 nm. The blue shift in the excitation profile makes the enhancement factor smaller at probe wavelengths of 225 and 238 nm. Therefore, the intensity loss of the W16 and W18 modes is associated with a blue shift in the excitation profile due to a reduction in hydrophobicity in the J and K states. The change in the dipole moment of retinal responding to the photoreaction would cause the changes in the transition dipole moment of tryptophan due to excitonic coupling.[71] This results in changes of the excitation profile and, thus, changes in the band intensities.

The negative band at the position of the W7 mode in Figure 1 had an asymmetric form compared to the UVRR band in the original state. The peak of this negative band was located around 1360 cm^{-1}, whereas the shoulder was detected at about 1340 cm^{-1}. The W7 mode is known to show a doublet arising from the Fermi resonance of the indole N_1-C_8 stretching with the combination bands of out-of-plane bending vibrations.[15] The intensity ratio of the two bands (I_{1360}/I_{1340}) is a marker of hydrophobicity around tryptophan. When the tryptophan residue is located in a hydrophobic environment, the intensity ratio becomes larger.[15,16,72] The spectral width of our laser was as wide as 20 cm^{-1}, so the tryptophan doublet band could not be resolved. The observation of a shoulder band at 1340 cm^{-1} on the band at 1360 cm^{-1} in the difference spectra may indicate that the I_{1360}/I_{1340} intensity ratio in the early photointermediate is smaller compared to that in the original state. Thus, the changes we observed in the intensities of W16 and W18 bands and the ratio of the W7 doublet suggest that the hydrophobicity of a tryptophan residue is reduced in the early picoseconds.

Under the 238 nm probe condition (Figure 3), the W3 mode exhibited a sigmoidal form arising from a wavenumber shift in the difference spectra at 5 ps. The W3 band is assigned to the C_2-C_3 stretching mode of the pyrrole ring,[15] and the wavenumber of the W3 mode is directly related to the side-chain conformation. The W3 wavenumber is correlated with the torsion angle, $\chi^{2,1}$, which is defined as the dihedral angle of the $C_2-C_3-C_\beta-C_\alpha$ linkage of the indole side chain.[16,73] The observed downshift implies a change in the torsion angle $\chi^{2,1}$ of the indole ring in the K state.

Changes in Protein Structure around the Tyrosine Residue. In the UVRR difference spectra probed at 238 nm, a large negative band instantaneously appeared at the position of the Y8a mode upon photoexcitation. Figure 4b shows that the bleached Y8a band partially recovered within the instrument response time and substantially recovered with a time constant of

30 ps. This indicated that the Y8a band intensity bleached in the J and K states and subsequently recovered in the "post-K" state. We extracted the contribution of Tyr174 to the band intensity in Figure 5b, showing that the Y8a band of Tyr174 was weakened in the J state and recovered in the K state. The Y8a mode is attributed to the in-plane stretching vibration on the phenyl ring.[15] The Raman intensity of this mode is resonantly enhanced by the Franck−Condon *A*-term mechanism via the L_a absorption (peak wavelength 222 nm). The maximum of its Raman excitation profile is around 225 nm.[74] Under the probe condition used in the present study, the intensity loss of the Y8a band arises from a blue shift of the Raman excitation profile. It has been reported that the L_a absorption band systematically blue-shifts when the tyrosine residue is in a more protic environment.[69] Therefore, the data of Figure 5b show that there is an increase in the hydrogen-bond strength of Tyr174 in the J state and a subsequent decrease in the K state. This is consistent with the FTIR observation that the hydrogen bond strength of Thr204 did not change between the original and K states in the absence of HtrII.[23]

Protein Response in the J and K States. The initial bleaching observed in all the tryptophan bands in the 225 nm spectra, as well as the bleaching observed in the Y8a band in the 238 nm spectra, is associated with the J state formation. Bleaching of the tryptophan bands is due to environmental changes occurring around the tryptophan residues, while the bleaching around the Y8a band can be attributed to a strengthening of the tyrosine hydrogen bond.

The 5 ps UVRR difference spectrum is assigned to the spectral change in the K state. In addition to the spectral changes observed in the J state, a lower wavenumber shift of the W3 band was observed in the K state in the time-resolved difference spectrum probed at 238 nm. Our data suggest that the orientation of the tryptophan side chain changes upon formation of the K state. In the K state, the chromophore is in the 13-cis form. The isomerization causes a significant structural change in the Schiff base region. The Trp171 side chain contacts the 9- and 13-methyl groups of retinal. Upon chromophore isomerization, the position of retinal's 13-methyl group changes compared to that in the all-trans configuration.[5] The displacement of the 13-methyl group would change the orientation of the side chain of Trp171. It is highly likely that the spectral change of the W3 band described above results from relief of the steric repulsion between retinal and Trp171.

Thus, as a whole, the spectral changes of SRII in the J and K states we observed are similar to those reported for BR.[21] However, the W16 and W18 bands probed at 238 nm exhibited a distinct difference in temporal evolution. Negative bands appeared within the instrument response time and became weaker within 10 ps in the SRII difference spectra, while no prominent band was observed during the first 10 ps for BR.[21] This difference indicates that the band intensity of the J state relative to the original state is smaller for SRII than it is for BR and suggests that the structure of Trp76 (Trp86 in BR) and/or Trp171 (Trp182 in BR) differs between the J states of the two proteins.

As shown in Figure 5b, the Y8a band bleached within the instrument response time and recovered within 10 ps, suggesting that the negative feature of the Y8a band for the Tyr174 residue derives from the J state of SRII. Together with the data for W16 and W18, it can be deduced that Tyr174, as well as Trp76 and/or Trp171, is perturbed upon the formation of the J state.

The maximum amplitude of the intensity change of the Y8a band in the UVRR difference spectra of SRII (Figures 3 and 4) was about 8 times larger than that of BR.[21] SRII and BR possess 10 and 11 tyrosines, respectively. If the structural change which gives rise to the same intensity change of the Y8a band took place both in SRII and BR, the difference of the relative intensity change would be as small as 10% between the two proteins. Thus, the prominent change of the Y8a band intensity observed in the present UVRR spectra of SRII suggests that the structural change of the protein moiety around retinal in SRII is much larger than that in BR. This is consistent with the previous FTIR study that the structural changes of protein moiety surrounding retinal chromophore in response to photoisomerization are spatially more extended in SRII than in BR.[9]

In Figure 5a, about 1/3 of the Y8a band intensity in the difference spectra at 1 ps consisted of the contribution of the spectral change due to Tyr174. Tyr185 in BR is conserved as Tyr174 in SRII. Even if a whole spectral change of Y8a band for BR is due to the structural change of Tyr185, the spectral change of Tyr174 in SRII is much larger than Tyr185 in the early picosecond time frame. As the Y8a band intensity is associated with changes in the hydrogen-bond strength,[69] the strengthening of the hydrogen bond of Tyr174 in SRII in the J state is larger than Tyr185 in BR. Y174F SRII does not function as a photosensor,[22] while Y185F BR pumps protons as well as WT BR.[75] The difference of the spectral changes between Tyr174 in SRII and Tyr185 in BR may correlate with the difference in the contribution to physiological functions of the two proteins.

FTIR study suggested that Tyr174 and Thr204, which are hydrogen-bonded to each other, are essential to the signal transduction and that a signal relay pathway starts with the steric conflict between the retinal $C_{14}H$ group and the side chain of Thr204 following retinal isomerization.[8] The FTIR data suggested that in this reaction the strength of hydrogen bond between Tyr174 and Thr204 changes. Thr204 in SRII is replaced as Ala215 at the same position in BR, which does not form a hydrogen bond to Tyr185. In addition, the BR triple mutant, P200T/V210Y/A215T, can activate HtrII and greatly enhance the phototaxis response.[33] It is highly likely that Tyr185 is hydrogen-bonded to Thr215 in this triple mutant and that the hydrogen-bond strength changes in accordance with the retinal isomerization. Actually, by using low-temperature FTIR spectroscopy, it has been reported that the hydrogen bond of the introduced Thr residue (i.e., A215T) strengthens by formation of the K intermediate due to the low-frequency shifts of the OH stretching mode. The frequency change in BR-T (105, 128, or 150 cm^{-1}) was similar to that in SRII (110 cm^{-1}).[76] Therefore, it is suggested that the intensity changes of the Y8a band due to Tyr174 in SRII and Tyr185 in BR can be correlated with the extent of the contribution to their physiological functions.

Recent ultrafast infrared spectroscopic experiments reported that protein backbone changes in the early picosecond time frame: protein bands appear in the amide I region within 0.3 ps and in the amide II region within 3 ps and decay partially in both regions with a time constants of 8−18 ps.[14] During the primary stages of the photocycle, changes in the amide II band of other microbial rhodopsins, blue and green proteorhodopsin, were also pointed out by low-temperature FTIR study.[77] The time constants of spectral changes detected by our UVRR measurements were different from those by these infrared studies. This is presumably because we observed the structural changes of different portion. Interestingly, the order of time constants of

the structural changes observed by both spectroscopies is the same. These studies revealed that the protein response to photoisomerization of the chromophore occurs in the J state and that the subsequent structural changes take place in a few tens of picoseconds.

In conclusion, the present data demonstrated that Tyr174 changes its structure and/or environment upon retinal isomerization. We also observed spectral changes associated with tryptophan residues in contact with the chromophore, presumably Trp76 and/or Trp171. Comparative studies of other retinal proteins will lead to a better understanding of the coupling between retinal isomerization and protein conformational changes. Our near future work involves the time-resolved UVRR measurements of the SRII−HtrII complex to understand the signal transduction of SRII in more detail.

■ ASSOCIATED CONTENT

Supporting Information. Table S1: vibrational normal modes and their descriptions of tryptophan and tyrosine Raman bands observed in Figures 1 and 3; Figure S1: picosecond time-resolved UVRR spectra of WT SRII and the Y174F mutant in the 650−2000 cm^{-1} region. This material is available free of charge via the Internet at http://pubs.acs.org.

■ AUTHOR INFORMATION

Corresponding Author

*Phone: +81-6-6850-5776. Fax: +81-6-6850-5776. E-mail: mztn@chem.sci.osaka-u.ac.jp.

Author Contributions

⊥These authors equally contributed to this work.

Funding Sources

This work was supported by a Grant-in-Aid for Scientific Research on the Priority Area Molecular Theory for Real Systems (Grant 20038037) from the Ministry of Education, Culture, Sports, Science and Technology of Japan (MEXT) to M.M. and a Grant-in-Aid for Scientific Research on the Priority Area Molecular Science for Supra Functional Systems from MEXT to Y.M. (Grant 19056013) and to Y.S. (Grants 20050012 and 22018010).

■ ABBREVIATIONS

BR,bacteriorhodopsin; HR,halorhodopsin; SRI,sensory rhodopsin I; SRII,sensory rhodopsin II; HtrII,halobacterial transducer protein II; TM2,second transmembrane helix; UVRR,ultraviolet resonance Raman; FTIR,Fourier transform infrared; DDM,*n*-dodecyl β-D-maltoside; IPTG,isopropyl 1-thio-β-galactoside; MES, 2(*N*-morpholino)ethanesulfonic acid; Tris,tris(hydroxymethyl) aminomethane.

■ REFERENCES

(1) Suzuki, D., Irieda, H., Homma, M., Kawagishi, I., and Sudo, Y. (2010) Phototactic and Chemotactic Signal Transduction by Transmembrane Receptors and Transducers in Microorganisms. *Sensors 10*, 4010–4039.

(2) Klare, J., Chizhov, I., and Engelhard, M. (2008) Microbial Rhodopsins: Scaffolds for Ion Pumps, Channels, and Sensors. *Results Probl. Cell Differ. 45*, 73–122.

(3) Spudich, J. L., Yang, C.-S., Jung, K.-H., and Spudich, E. N. (2000) RETINYLIDENE PROTEINS: Structures and Functions from Archaea to Humans. *Annu. Rev. Cell Dev. Biol. 16*, 365–392.

(4) Gordeliy, V. I., Labahn, J., Moukhametzianov, R., Efremov, R., Granzin, J., Schlesinger, R., Buldt, G., Savopol, T., Scheidig, A. J., Klare, J. P., and Engelhard, M. (2002) Molecular basis of transmembrane signalling by sensory rhodopsin II-transducer complex. *Nature 419*, 484–487.

(5) Luecke, H., Schobert, B., Lanyi, J. K., Spudich, E. N., and Spudich, J. L. (2001) Crystal Structure of Sensory Rhodopsin II at 2.4 Angstroms: Insights into Color Tuning and Transducer Interaction. *Science 293*, 1499–1503.

(6) Sasaki, J., and Spudich, J. L. (2008) Signal Transfer in Haloarchaeal Sensory Rhodopsin− Transducer Complexes. *Photochem. Photobiol. 84*, 863–868.

(7) Hein, M., Wegener, A. A., Engelhard, M., and Siebert, F. (2003) Time-Resolved FTIR Studies of Sensory Rhodopsin II (NpSRII) from *Natronobacterium pharaonis*: Implications for Proton Transport and Receptor Activation. *Biophys. J. 84*, 1208–1217.

(8) Ito, M., Sudo, Y., Furutani, Y., Okitsu, T., Wada, A., Homma, M., Spudich, J. L., and Kandori, H. (2008) Steric Constraint in the Primary Photoproduct of Sensory Rhodopsin II Is a Prerequisite for Light-Signal Transfer to HtrII. *Biochemistry 47*, 6208–6215.

(9) Kandori, H., Shimono, K., Sudo, Y., Iwamoto, M., Shichida, Y., and Kamo, N. (2001) Structural Changes of pharaonis Phoborhodopsin upon Photoisomerization of the Retinal Chromophore: Infrared Spectral Comparison with Bacteriorhodopsin. *Biochemistry 40*, 9238–9246.

(10) Furutani, Y., Kamada, K., Sudo, Y., Shimono, K., Kamo, N., and Kandori, H. (2005) Structural Changes of the Complex between pharaonis Phoborhodopsin and Its Cognate Transducer upon Formation of the M Photointermediate. *Biochemistry 44*, 2909–2915.

(11) Moukhametzianov, R., Klare, J. P., Efremov, R., Baeken, C., Göppner, A., Labahn, J., Engelhard, M., Büldt, G., and Gordeliy, V. I. (2006) Development of the signal in sensory rhodopsin and its transfer to the cognate transducer. *Nature 440*, 115–119.

(12) Lutz, I., Sieg, A., Wegener, A. A., Engelhard, M., Boche, I., Otsuka, M., Oesterhelt, D., Wachtveitl, J., and Zinth, W. (2001) Primary reactions of sensory rhodopsins. *Proc. Natl. Acad. Sci. U.S.A. 98*, 962–967.

(13) Imamoto, Y., Shichida, Y., Hirayama, J., Tomioka, H., Kamo, N., and Yoshizawa, T. (1992) Nanosecond Laser Photolysis of Phoborhodopsin: from *Natronobacterium pharaonis* Appearance of KL and L Intermediates in the Photocycle at Room Temperature. *Photochem. Photobiol. 56*, 1129–1134.

(14) Gross, R., Wolf, M. M. N., Schumann, C., Friedman, N., Sheves, M., Li, L., Engelhard, M., Trentmann, O., Neuhaus, H. E., and Diller, R. (2009) Primary Photoinduced Protein Response in Bacteriorhodopsin and Sensory Rhodopsin II. *J. Am. Chem. Soc. 131*, 14868–14878.

(15) Harada, I., Takeuchi, H. (1986) Raman and Ultraviolet Resonance Raman Spectra of Proteins and Related Compounds, in *Spectroscopy of Biological Systems* (Clark, R. J. H., Hester, R. E., Eds.), pp 113−175, John Wiley & Sons, Chichester.

(16) Kitagawa, T., Hirota, S. (2002) Raman Spectroscopy of Proteins, in *Handbook of Vibrational Spectroscopy* (Chalmers, J. M., Griffiths, P. R., Eds.), pp 3426−3446, John Wiley & Sons, Chichester.

(17) Sato, A., Gao, Y., Kitagawa, T., and Mizutani, Y. (2007) Primary protein response after ligand photodissociation in carbonmonoxy myoglobin. *Proc. Natl. Sci. Acad. Sci. U.S.A. 104*, 9627–9632.

(18) Sato, A., and Mizutani, Y. (2005) Picosecond Structural Dynamics of Myoglobin following Photodissociation of Carbon Monoxide As Revealed by Ultraviolet Time-Resolved Resonance Raman Spectroscopy. *Biochemistry 44*, 14709–14714.

(19) Mizuno, M., Hamada, N., Tokunaga, F., and Mizutani, Y. (2007) Picosecond Protein Response to the Chromophore Isomerization of Photoactive Yellow Protein: Selective Observation of Tyrosine and Tryptophan Residues by Time-Resolved Ultraviolet Resonance Raman Spectroscopy. *J. Phys. Chem. B 111*, 6293–6296.

(20) Fujiwara, A., and Mizutani, Y. (2008) Photoinduced electron transfer in glucose oxidase: a picosecond time-resolved ultraviolet resonance Raman study. *J. Raman Spectrosc. 39*, 1600–1605.

(21) Mizuno, M., Shibata, M., Yamada, J., Kandori, H., and Mizutani, Y. (2009) Picosecond Time-Resolved Ultraviolet Resonance Raman Spectroscopy of Bacteriorhodopsin: Primary Protein Response to the Photoisomerization of Retinal. *J. Phys. Chem. B 113*, 12121–12128.

(22) Sudo, Y., Furutani, Y., Kandori, H., and Spudich, J. L. (2006) Functional Importance of the Interhelical Hydrogen Bond between Thr204 and Tyr174 of Sensory Rhodopsin II and Its Alteration during the Signaling Process. *J. Biol. Chem. 281*, 34239–34245.

(23) Sudo, Y., Furutani, Y., Shimono, K., Kamo, N., and Kandori, H. (2003) Hydrogen Bonding Alteration of Thr-204 in the Complex between pharaonis Phoborhodopsin and Its Transducer Protein. *Biochemistry 42*, 14166–14172.

(24) Kitajima-Ihara, T., Furutani, Y., Suzuki, D., Ihara, K., Kandori, H., Homma, M., and Sudo, Y. (2008) Salinibacter Sensory Rhodopsin. *J. Biol. Chem. 283*, 23533–23541.

(25) Kaminaka, S., and Mathies, R. A. (1998) High-Throughput Large-Aperture Prism Prefilter for Ultraviolet Resonance Raman Spectroscopy. *Appl. Spectrosc. 52*, 469–473.

(26) Sweeney, J. A., and Asher, S. A. (1990) Tryptophan UV Resonance Raman Exsitation Profiles. *J. Phys. Chem. 94*, 4784–4791.

(27) Doig, S. J., Reid, P. J., and Mathies, R. A. (1991) Picosecond Time-Resolved Resonance Raman Spectroscopy of Bacteriorhodopsin's J, K, and KL Intermediates. *J. Phys. Chem. 95*, 6372–6379.

(28) Herbst, J., Heyne, K., and Diller, R. (2002) Femtosecond Infrared Spectroscopy of Bacteriorhodopsin Chromophore Isomerization. *Science 297*, 822–825.

(29) Terentis, A. C., Ujj, L., Abramczyk, H., and Atkinson, G. H. (2005) Primary events in the bacteriorhodopsin photocycle: Tortional vibrational dephasing in the first excited electronic state. *Chem. Phys. 313*, 51–62.

(30) Kandori, H., Furutani, Y., Shimono, K., Shichida, Y., and Kamo, N. (2001) Internal Water Molecules of pharaonis Phoborhodopsin Studied by Low-Temperature Infrared Spectroscopy. *Biochemistry 40*, 15693–15698.

(31) Hirayama, J., Imamoto, Y., Shichida, Y., Kamo, N., Tomioka, H., and Yoshizawa, T. (1992) Photocycle of phoborhodopsin from haloalkaliphilic bacterium (Natronobacterium pharaonis) studied by low-temperature spectrophotometry. *Biochemistry 31*, 2093–2098.

(32) Sudo, Y., Furutani, Y., Wada, A., Ito, M., Kamo, N., and Kandori, H. (2005) Steric Constraint in the Primary Photoproduct of an Archaeal Rhodopsin from Regiospecific Perturbation of C-D Stretching Vibration of the Retinyl Chromophore. *J. Am. Chem. Soc. 127*, 16036–16037.

(33) Sudo, Y., and Spudich, J. L. (2006) Three strategically placed hydrogen-bonding residues convert a proton pump into a sensory receptor. *Proc. Natl. Acad. Sci. U.S.A. 103*, 16129–16134.

(34) He, Y., Krebs, M. P., Fischer, W. B., Khorana, H. G., and Rothschild, K. J. (1993) FTIR Difference Spectroscopy of the Bacteriorhodopsin Mutant Tyr- 185-Phe: Detection of a Stable 0-like Species and Characterization of Its Photocycle at Low Temperature. *Biochemistry 32*, 2282–2290.

(35) Wegener, A.-A., Chizhov, I., Engelhard, M., and Steinhoff, H.-J. (2000) Time-resolved detection of transient movement of helix F in spin-labelled pharaonis sensory rhodopsin II. *J. Mol. Biol. 301*, 881–891.

(36) Wegener, A.-A., Klare, J. P., Engelhard, M., and Steinhoff, H.-J. (2001) Structural insights into the early steps of receptor−transducer signal transfer in archaeal phototaxis. *EMBO J. 20*, 5312–5319.

(37) Koch, M. H., Dencher, N. A., Oesterhelt, D., Plöhn, H. J., Rapp, G., and Büldt, G. (1991) Time-resolved X-ray diffraction study of structural changes associated with the photocycle of bacteriorhodopsin. *EMBO J. 10*, 521–526.

(38) Subramaniam, S., Gerstein, M., Oesterhelt, D., and Henderson, R. (1993) Electron diffraction analysis of structural changes in the photocycle of bacteriorhodopsin. *EMBO J. 12*, 1–8.

(39) Rothschild, K. J., Braiman, M. S., Mogi, T., Stern, L. J., and Khorana, H. G. (1989) Conserved amino acids in F-helix of bacteriorhodopsin form part of a retinal binding pocket. *FEBS Lett. 250*, 448–452.

(40) Brack, T. L., and Atkinson, G. H. (1989) Picosecond time-resolved resonance Raman spectrum of the K-590 intermediate in the room temperature bacteriorhodopsin. *J. Mol. Struct. 214*, 289–303.

(41) Hsieh, C.-L., Nagumo, M., Nicol, M., and El-Sayed, M. A. (1981) Picosecond and Nanosecond Resonance Raman Studies of bancteriorhodopsin. Do Configurational Changes of Retinal Occur in Picoseconds? *J Phys. Chem. 85*, 2714–2717.

(42) Smith, S. O., Lugtenburg, J., and Mathies, R. A. (1985) Determination of Retinal Chromophore Structure in Bacteriorhodopsine with Resonance Raman Spectroscopy. *J. Membr. Biol. 85*, 95–109.

(43) Terner, J., Hsieh, C.-L., Burns, A. R., and El-Sayed, M. A. (1979) Time-resolved resonance Raman spectroscopy of intermediates of bacteriorhodopsin: The bK_{590} intermediate. *Proc. Natl. Sci. Acad. Sci. U.S.A. 76*, 3046–3050.

(44) Weidlich, O., Ujj, L., Jäger, F., and Atkinson, G. H. (1997) Nanosecond Retinal Structure Changes in K-590 During the Room-Temperature Bacteriorhodopsin Photocycle: Picosecond Time-Resolved Coherent Anti-Stokes Raman Spectroscopy. *Biophys. J. 72*, 2329–2341.

(45) Diller, R., Iannone, M., Cowen, B. R., Maiti, S., Bogomolin, R. A., and Hochstrasser, R. M. (1992) Picosecond Dynamics of Bacteriorhodopsin, Probed by Time-Resoleved Infrared Spectroscopy. *Biochemistry 31*, 5567–5572.

(46) Diller, R., Maiti, S., Walker, G. C., Cowen, B. R., Pippenger, R., Bogomolin, R. A., and Hochstrasser, R. M. (1995) Femtosecond time-resolved infrared laser study of the J-K transition of bacteriorhodopsin. *Chem. Phys. Lett. 241*, 109–115.

(47) Dioumaev, A. K., and Braiman, M. S. (1997) Two Bathointermediates of the Bacteriorhodopsin Photocycle, Distinguished by Nanosecond Time-Resoleved FTIR Spectroscopy at Room Temperature. *J. Phys. Chem. B 101*, 1655–1662.

(48) Hage, W., Kim, M., Frei, H., and Mathies, R. A. (1996) Protein Dynamics in the Bacteriorhodopsine Photocycle: A Nanosecond Step-Scan FTIR Investigation of the KL to L Transition. *J. Phys. Chem. 100*, 16026–16033.

(49) Sasaki, J., Maeda, A., Kato, C., and Hamaguchi, H.-o. (1993) Time-Resolved Infrared Spectral Analysis of the KL-to-L Conversion in the Photocycle of Bacteriorhodopsin. *Biochemistry 32*, 867–871.

(50) Weidlich, O., and Siebert, F. (1993) Time-Resolved Step-Scan FT-IR Investigations of the Transition from KL to L in the Bacteriorhodopsin Photocycle: Indentification of Chromophore Twists by Assigning Hydrogen-Out-Of-Plane (HOOP) Bending Vibrations. *Appl. Spectrosc. 47*, 1394–1400.

(51) Braiman, M., and Mathies, R. (1982) Resonance Raman spectra of bacteriorhodopsin's primary photoproduct: Evidence for a distorted 13-cis retinal chromophore. *Proc. Natl. Sci. Acad. Sci. U.S.A. 79*, 403–407.

(52) Kandori, H., Belenky, M., and Herzfeld, J. (2002) Vibrational Frequency and Dipolar Orientation od the Protonated Schiff Base in bacteriorhodopsin before and after Photoisomerization. *Biochemistry 41*, 6026–6031.

(53) Kandori, H., Kinoshita, N., Shichida, Y., and Maeda, A. (1998) Protein Structural Changes in Bacteriorhodopsin upon Photoisomerization As Revealed by Polarized FTIR Spectroscopy. *J. Phys. Chem. B 102*, 7899–7905.

(54) Kandori, H., Kinoshita, N., Yamazaki, Y., Maeda, A., Shichida, Y., Needleman, R., Lanyi, J. K., Bizounok, M., Herzfeld, J., Raap, J., and Lugtenburg, J. (1999) Structural Change of Threonine 89 upon Photoisomerization in Bacteriorhodopsin As Reveald by Polarized FTIR Spectroscopy. *Biochemistry 38*, 9676–9683.

(55) Kandori, H., Kinoshita, N., Yamazaki, Y., Maeda, A., Shichida, Y., Needleman, R., Lanyi, J. K., Bizounok, M., Herzfeld, J., Raap, J., and Lugtenburg, J. (2000) Local and distant protein structural changes on photoisomerization of the retinal in bacteriorhodopsin. *Proc. Natl. Sci. Acad. Sci. U.S.A. 97*, 4643–4648.

(56) Kandori, H., and Shichida, Y. (2000) Direct Observation of the Bridged Water Stretching Vibrations Inside a Protein. *J. Am. Chem. Soc. 122*, 11745–11746.

(57) Kandori, H., Yamazaki, Y., Shichida, Y., Raap, J., Lugtenburg, J., Belenky, M., and Herzfeld, J. (2001) Tight Asp-85-Thr-89 association during the pump switch of bacteriorhodopsin. *Proc. Natl. Sci. Acad. Sci. U.S.A. 98*, 1571–1576.

(58) Rothchild, K. J., Roepe, P., and Gillespie, J. (1985) Fourier transform infrared spectroscopic evidence for the existence of two conformations of the bacteriorhodopsin primary photoproduct at low temperature. *Biochim. Biophys. Acta 808*, 140–148.

(59) Shibata, M., and Kandori, H. (2005) FTIR Studies of Internal Water Molecules in the Schiff Base Region of Bacteriorhodopsin. *Biochemistry 44*, 7406–7413.

(60) Tanimoto, T., Furutani, Y., and Kandori, H. (2003) Structural Changes of Water in the Schiff Base Region of Bacteriorhodopsin: Proposal of a Hydration Switch Model. *Biochemistry 42*, 2300–2306.

(61) Lanyi, J. K., and Schobert, B. (2003) Mechanisem of Proton Transport in Bacteriorhodopsin from Crystallographic Structures of the K, L, M_1, M_2, and M_2' Intermediates of the Photocycle. *J. Mol. Biol. 328*, 439–450.

(62) Schobert, B., Cupp-Vickery, J., Harnak, V., Smith, S. O., and Lanyi, J. K. (2002) Crystallographic Structure of the K intermediate of Bacteriorhodopsin: Conservation of Free Energy after Photoisomerization of the Retinal. *J. Mol. Biol. 321*, 715–726.

(63) Hayashi, S., Tajkhorshid, E., Kandori, H., and Schulten, K. (2004) Role of Hydrogen-Bond Network in Energy Storage of Bacteriorhodopsin's Light-Driven Proton Pump Revealed by ab initio Normal-Mode Analysis. *J. Am. Chem. Soc. 126*, 10516–10517.

(64) Hayashi, S., Tajkhorshid, E., and Schulten, K. (2002) Structural Changes during the Formation of Early Intermediates in the Bacteriorhodopsin Photocycle. *Biophys. J. 83*, 1281–1297.

(65) Braiman, M. S., Mogi, T., Stern, L. J., Hackett, N. R., Chao, B. H., Khorana, H. G., and Rothschild, K. J. (1988) Vibrational Spectroscopy of Bacteriorhodopsin Mutants: I. Tyrosine-I85 Protonates and Deprotonates During the Photocycle. *Proteins: Struct., Funct., Genet. 3*, 219–229.

(66) Rothschild, K. J., Roepe, P., Ahl, P. L., Earnest, T. N., Bogomolni, R. A., Gupta, S. K. D., Mulliken, C. M., and Herzfeld, J. (1986) Evidence for a tyrosine protonation change during the primary phototransition of bacteriorhodopsin at low temperature. *Proc. Natl. Acad. Sci. U.S.A. 83*, 347–351.

(67) Asher, S. A., Ludwig, M., and Johnson, C. R. (1986) UV Resonance Raman Excitation Profiles of the Aromatic Amino Acids. *J. Am. Chem. Soc. 108*, 3186–3197.

(68) Rava, R. P., and Spiro, T. G. (1985) Resonance Enhancement in the Ultraviolet Raman Spectra of Aromatic Amino Acids. *J. Phys. Chem. 89*, 1856–1861.

(69) Chi, Z., and Asher, S. A. (1998) UV Raman Determination of the Environment and Solvent Exposure of Tyr and Trp Residues. *J. Phys. Chem. B 102*, 9595–9602.

(70) Matsuno, M., and Takeuchi, H. (1998) Effects of Hydrogen Bonding and Hydrophobic Interactions on the Ultraviolet Resonance Raman Intensities of Indole Ring Vibrations. *Bull. Chem. Soc. Jpn. 71*, 851–857.

(71) Schenkl, S., Mourik, F. v., Zwan, G. v. d., Haacke, S., and Chergui, M. (2005) Probing the Ultrafast Change Translocation of Photoexcited Retinal in Bacteriorhodopsin. *Science 309*, 917–920.

(72) Harada, I., Yamaguchi, T., Uchida, K., and Takeuchi, H. (1990) Ultraviolet Resonance Raman Spectra of Bacteriorhodopsin in the Light-Adapted and Dark-Adapted States. *J. Am. Chem. Soc. 112*, 2443–2445.

(73) Miura, T., Takeuchi, H., and Harada, I. (1989) Tryptophan Raman Bands Selective to Hydrogen Bonding and Side-Chain Conformation. *J. Raman Spectrosc. 20*, 667–671.

(74) Ludwig, M., and Asher, S. A. (1988) Ultraviolet Resonance Raman Excitation Profiles of Tyrosine: Dependence of Raman Cross Sections on Excited-State Intermediates. *J. Am. Chem. Soc. 110*, 1005–1011.

(75) Mogi, T., Stern, L. J., Hackett, N. R., and Khorana, H. G. (1987) Bacteriorhodopsin mutants containing single tyrosine to phenylalanine substitutions are all active in proton translocation. *Proc. Natl. Acad. Sci. U.S.A. 84*, 5595–5599.

(76) Sudo, Y., Furutani, Y., Spudich, J. L., and Kandori, H. (2007) Early Photocycle Structural Changes in a Bacteriorhodopsin Mutant Engineered to Transmit Photosensory Signals. *J. Biol. Chem. 282*, 15550–15558.

(77) Amsden, J. J., Kralj, J. M., Bergo, V. B., Spudich, E. N., Spudich, J. L., and Rothschild, K. J. (2008) Different Structural Changes Occur in Blue- and Green-Proteorhodopsins during the Primary Photoreaction. *Biochemistry 47*, 11490–11498.